Measures and Indices for Intrinsic Characterization of Cardiac Dysfunction during Filling & Systolic Ejection

Zhong, Liang; Ghista, Dhanjoo N.; Lim, Soo Teik; Chua, Siang Jin; Ng, Yin Kwee

2005

Zhong, L., Ghista, D. N., Ng, Y. K., Lim, S. T., & Chua, S. J. (2005). Measures and Indices for Intrinsic Characterization of Cardiac Dysfunction during Filling & Systolic Ejection. Journal of Mechanics in Medicine and Biology, 5(2), 307-332.

https://hdl.handle.net/10356/82765

https://doi.org/10.1142/S0219519405001369

Measures and Indices for Intrinsic Characterization of Cardiac Dysfunction during Filling & Systolic Ejection

E. Y-K. Ng, Dhanjoo N. Ghista, Liang Zhong,

Lim Soo Teik [#] and Chua Siang Jin [#]

College of Engineering, School of Mechanical and Production Engineering,
Nanyang Technological University, 50 Nanyang Avenue, Singapore 639798

[#] Department of Cardiology, National Heart Center, SingHealth, Mistri Wing,
3rd Hospital Avenue, Singapore 168752

Abstract

The paper discusses the development and application of bioengineering indices for reliable diagnosis of cardiac functional modalities in filling and contraction phases.

During diastolic filling, the left-ventricular (LV) volume developed is a response to LV suction at early rapid filling and LA contraction at late filling. However in LV ejection, the LV flow-rate and aortic pressure constitute response to LV myocardial stress and intra-LV pressure generation. The differential equations used in the governing of these relationships have been developed. By matching the solutions of these differential equations with the clinical data of LV volume and pressure, we can determine the heart model 'differential equations' parameters, as well as the derived indices. These parameters and indices include: compliance and resistance-to-filling for characterizing diastolic-filling function, together with the index of LV contractility (in terms of maximum LV contractile power and stress-velocity relationship for contractile element). By evaluating them, it is possible to diagnose more reliably and differentially heart diseases due to an increase in filling-resistance and contractility abnormalities.

Keywords: Heart Failure, Ventricular Function, Angiography, Noninvasive, Contractility, Resistance.

1. Introduction

Heart failure is a leading cause of death in developed countries, including Singapore. This clinical syndrome may be a manifestation of increased LV elastance (or decreased LV compliance) and diminished LV myocardial contractility. Hypertension is one of the many causes of increased LV elastance. Myocardial ischemia or infarction, myocarditis, other myocardial diseases, as well as electrical conduction abnormality, can result in impaired LV contractility. We hence want to gain insight into these phenomena by means of somewhat simplistic and effective model using physiological indices to characterize these phenomena.

Characterizing the LV as a pump requires one to account for both passive and active myocardial properties, and the associated preload and afterload in particular. We, however, would like to characterize the LV pump function in terms of its intrinsic parameters, independent of preload and afterload. For decades, many cardiologists and biomedical engineers have been attempting to quantify the cardiac compliance and resistance-to-filling as well as cardiac contractility, so as to apply them clinically. We have addressed this need in this paper, which allows convenient and reliable diagnosis of cardiac disorders, by formulating and evaluating some novel physiological performance indices. In this aspect, we have (i) modeled the relationship between LV pressure and volume during filling and ejection phases, (ii) provided application of the presently proposed heart model to the actual patient data, (iii) demonstrated evaluation of the model parameters and indices, and (iv) made inferences to how those indices can help in diagnosing cardiac disorders.

2. History of Research in this Field

Clinicians have been using simple clinical measurements such as blood pressure and electrocardiogram to diagnose cardiac pathologies. Subsequently, biomedical engineers developed pattern-recognitions techniques to help clinicians interpret ECG measurements.

However, we need to model and parametrize the intrinsic functions of the heart (in particular the LV), so as to provide clinical inferences.

In a bioengineering sense, the heart can be described as a source of blood pressure and its biomechanical behavior can be understood in terms of the time-varying relationship between ventricular blood cavity volume and pressure. For many years, clinicians have used this relationship as a measure of cardiac function (Grodins, 1959; Elzinga, 1972; Suga and Sagawa, 1974; Vaartjes and Boom, 1987; Palladino, 1998). No doubt, LV pressure and volume are the fundamental physical variables used to describe indirectly the biomechanical properties of LV. However, a more intrinsic understanding of LV mechanisms can be obtained in terms of LV myocardial properties to characterize the underlying ventricular pump function, as exemplified by the concept of LV myocardial stress and modulus, put forth by Ghista et al. (1969, 1970), to characterize both diastolic and systolic performance. Some of these earlier works in this intrinsic characterization of LV function (Ghista, 1969 & 1975) have in fact been adopted clinically.

2.1 LV Diastolic Dysfunction Characterization:

The heart may be conceived as a pump that receives blood from a low-pressure system and raises it to a high-pressure system. With periodic stimulation of its muscles, it contracts and pumps blood throughout the body. In diastole, the ventricular wall must be compliant to allow rapid and complete filling process at low filling pressure. Impaired capacity to fill the LV results in diastolic dysfunction.

In recent years, there is increased awareness of the clinical importance of LV diastolic dysfunction (Mirsky, 1974). This impairment of LV diastolic function is associated with diseases such as myocardial infarct and hypertrophy (Dougherty, 1984; Little, 1990; Yellin, 1990). This underscores the need for biomechanical characterization of LV diastolic dysfunction.

2.2 LV Systolic Dysfunction Assessment:

'How to intrinsically assess the systolic function of the LV' has long been the major problem in physiology and cardiology, and this problem remains yet unsolved. The systolic function of the LV has been viewed at different levels (Frank, 1895, Starling, 1918). Way back in 1895, Frank characterized ventricular function in terms of the pressure-volume diagram. In 1918, Starling first viewed the LV as a pump to generate cardiac output (proportional to its filling) against an afterload. Hill (1938) and Huxley (1957, 1974) investigated muscle contraction by means of muscle force-velocity relationship at the micro-structural level (cross-bridge theory). Then, more recently, Suga (1993) proposed that the systolic function of the LV is a process of converting cross-bridge chemical energy into the mechanical energy during contraction.

In systole, the ventricular wall myocardium must generate adequate force to build sufficient pressure to open the aortic valve, and shorten (and thicken) the LV wall to pump an appropriate stroke volume. Therefore, systolic dysfunction is the inability of the myocardium to shorten against the aortic pressure load, characterizing LV disability to eject blood into a high-pressure aorta.

3. Justification for Clinical Indices of Cardiac Function

LV end-diastolic filling-pressure and volume characterize the elastance during the diastolic phase. Although the concept of myocardium compliance was introduced in the 60(s), in attempt to quantify the diastolic pressure-volume relationship (Warner, 1959; Defares, 1963; Suga, 1969; Mirsky, 1976), ~~but~~ there continues to be a need to elaborate the relationship between LV diastolic pressure and volume in terms of the intrinsic parameters of LV function.

For LV systolic function, cardiologists use the term contractility loosely to denote the capacity of the heart (LV) to generate an appropriate pressure. Many factors, such as

myocardial ischemia and electrical conduction disorders, affect LV contractility. However, hitherto, we do not have a reliable index of contractility to quantify contractility in normal and failing hearts. In one-dimensional muscular biomechanics, contractility embodies the muscle force-length relation during isometric contraction and force-velocity-length relation during shortening. However, this can be done only in the experimental animals, with one-dimensional muscle preparations. The work on in-vivo measures of cardiac contractility has in fact been pioneered by Ghista et al. (1980, 1987), by modeling and quantifying LV intra-myocardial mechanics as well as intra-LV fluid-flow.

4. Research Methodology

The methodology delineated in this paper comprises the following steps:

1. In both the filling and ejection phases, we monitor the patients' LV pressure and volume, by LV catheterization and cineventriculographic analysis using the Pie Medical Imaging's CAAS II QCA/LVA software (2003). The subject in this study was studied in a resting recumbent (baseline) state, after premedication with 100-500 mg of sodium pentobarbital by retrograde aortic catheterization. The LV chamber pressure was measured by a pigtail catheter and Statham P23Eb pressure transducer; the pressure was recorded immediately during angiocardiography. Angiography was performed by injecting 30-36 ml of 75% sodium diatrizoate into the LV at 10 to 12 ml/s. Monoplane cineangiocardiograms were recorded in a RAO 30° projection from a 9" image intensifier using 35 mm film at 50 frames/s using INTEGRIS Allura 9 system.
2. Carry out analysis of (i) filling process during the filling phase (ii) volume response to generated LV wall stress during the systolic phase.
3. Develop models for the filling and systolic phases and relate both the LV pressure and volume.

4. Match the differential equations model solutions with the clinical (non-invasively determinable using a wrist watch-like Pulse Analyzer device, 2003) data, and evaluate the model parameters representing filling and ejection phases.
5. Formulate and calculate indices for both diastolic-filling and systolic-ejection phases in terms of the model parameters.

The innovation of this work lies in the (i) filling and systolic-ejection processes modeling and identification of the model parameters, (ii) formulation of integrated diagnostic-indices to characterize filling and ejection phases dysfunctions, (iii) clinical applicability of these indices in disease diagnosis.

5. LV Myocardial Properties & Intra-LV Blood-flow

5.1 State of the Art and its Shortcomings:

Traditionally, the major determinants of LV pump function have been end-diastolic pressure, stroke-volume and ejection fraction (EF). However, these determinants do not intrinsically assess LV pump function or dysfunction, in the form of LV resistance-to-filling (LV-RTF) and contractility (LV-CONT).

In clinical practice, demonstration of ischemic but viable myocardium is useful in deciding candidacy for revascularization procedure such as coronary bypass surgery or coronary angioplasty. Improved LV wall motion and ejection-fraction (EF) following administration of nitroglycerin, dobutamine, or other appropriate pharmacologic agents, are often employed as indirect indicators of myocardium viability. However, because LV wall motion and EF are not intrinsic indicators of LV-RTF and LV-CONT, they do not indicate if, following coronary bypass surgery, the myocardium will contribute to the improvement of the ventricular pumping efficiency with:

- decreased LV-RTF, in terms of reduced intra-LV (mitral valve-to-apex) pressure-gradient,

- and a more favorable LV-CONT, in terms of better intra-LV apex-to-aortic valve pressure-gradient during ejection.

5.2 LV Myocardial Constitutive Properties:

For assessment of the LV as a blood pump, instead of the traditional global measurement of stroke-volume (and stroke-power), we have determined (Ghista 1971, 1973 & 1974):

- the stiffness of the pressurized spherical-model of LV during the filling phase as an index of LV-RTF,
- and of its wall stress (σ) vs. strain-rate ($\dot{\varepsilon}$) as a measure of LV-CONT.

Figure 1 depicts cineangiographically-derived LV pressure vs. time, and LV spherical model dimensions, equivalent radius R [$=(3\times LV\ \text{volume}/4\pi)^{1/3}$] and wall-thickness h, during a cardiac cycle. In this figure, 1-20 is diastolic filling phase; 20-23 is isovolumic contraction phase; 23-35 is ejection phase, 35-40 is isovolumic relaxation phase. This data is employed to compute (i) elastic-modulus LV (E) vs. wall stress (σ) during the filling phase, and (ii) LV wall-stress (σ) vs. strain-rate ($\dot{\varepsilon}$) during the ejection phase.

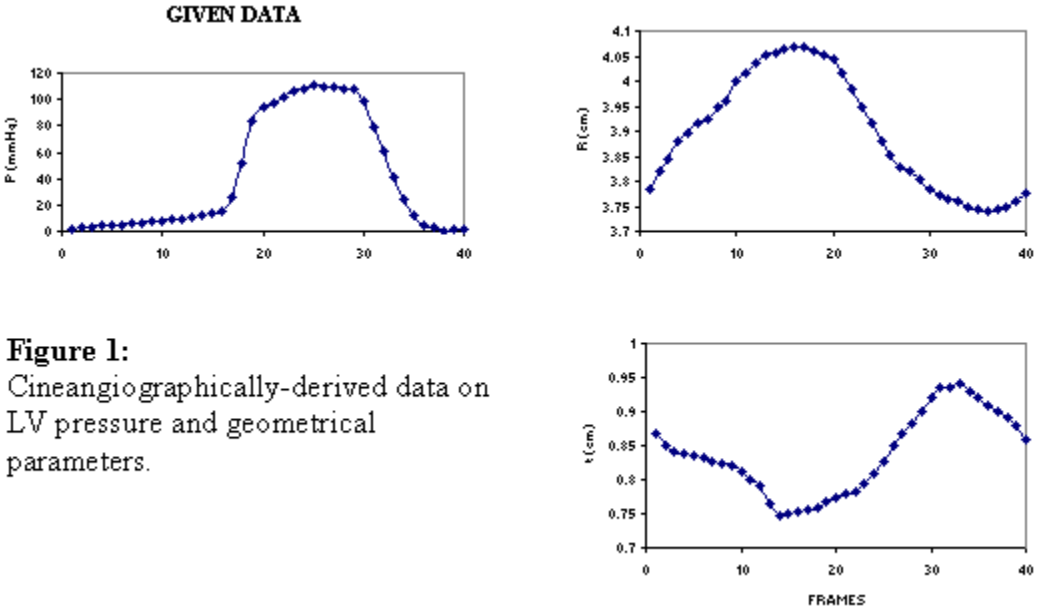

Figure 1:
Cineangiographically-derived data on LV pressure and geometrical parameters.

FILLING PHASE: E Vs. σ

EJECTION PHASE: σ vs. $\dot{\varepsilon}$

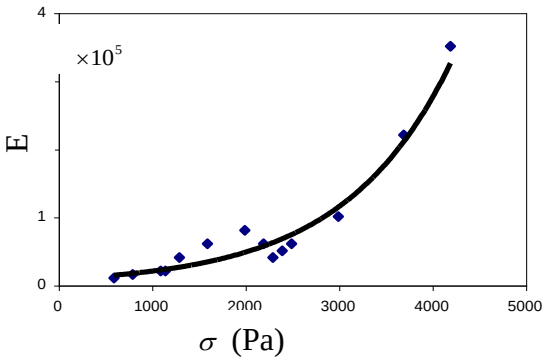

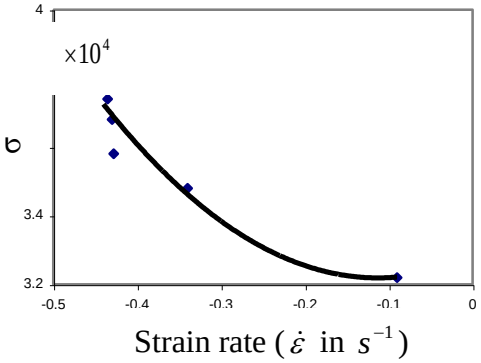

2-a: Clinical measure of LV filling-phase stiffness

2-b: Clinical measure of LV myocardial stress vs. strain-rate ($\cong$ LV myocardial contractility)

Figure 2: Computed (i) LV E vs. σ during diastole and (ii) σ vs. $\dot{\varepsilon}$.

Figures 2 (a & b) depict LV elastic modulus (E) vs. wall stress (σ) during the filling phase, and σ vs. $\dot{\varepsilon}$ during the ejection phase. Note that we are obtaining (for the first time) an in-vivo inverse relationship between σ & $\dot{\varepsilon}$, analogues to the 1-D in-vitro experimental observation of 'force vs. velocity' of isolated muscle preparation.

5.3 Intra-LV of Blood-flow Velocity and Pressure Distribution (to characterize resistance-to-filling and contractility).

The data required for the FEA (finite-element analysis) consists of:

- LV 2-D long-axis frames during LV diastolic and systolic phases,
- LV pressure vs. time, associated with these LV frames,
- Computation of LV instantaneous wall velocities as well as instantaneous velocity of blood entering the LV during the filling phase and leaving the LV during the ejection phase.

From this FEA, we have carried out computational solution of $\nabla^2\Phi$ (Φ being the velocity potential), to obtain the instantaneous distributions of intra-LV blood-flow velocity and differential-pressure during filling and ejection phases, to thereby

intrinsically characterize LV-RTF and LV-CONT respectively. The analysis is detailed in Subbaraj (1987).

Further, by comparing intra-LV pressure-gradient before and after administration of nitroglycerin (a myocardial perfusing agent, and hence a quasi-simulator of augmented perfusion of the ischemic myocardium, due to coronary bypass surgery), we can infer how the myocardium is going to respond and how these LV functional indices will improve after coronary bypass surgery.

5.3.1 Candidacy for coronary-bypass surgery:

The ideal situation is for the LV wall contraction to be so graded (from LV apex to the base) ~~in~~ such that adequate flow is generated in the apical region and a near-uniform flow is maintained throughout the LV chamber. The factors contributing to adequate intra-LV flow and cardiac output, with a smooth washout, are strong LV wall contraction and uniformly accelerating wall motion. If following administration of nitroglycerin (a myocardial perfusing agent, and hence a quasi-simulator of coronary bypass surgery or coronary angioplasty), the LV wall can contract more uniformly and thereby set up a more favourable intra-LV velocity field (instead of a regional pattern of compensatory regional hypercontractility and associated high wall tension and oxygen demand to make up for a region of hypocontractility), then such a patient would be a good candidate for coronary bypass surgery.

Referring to **Figure 3**, for the patient (with a myocardial infarct) TURN, Figures ($3a_1$ & a_2) depict super-imposed LV outlines during diastole and systole, before nitroglycerin administration (a_1) and after nitroglycerin administration (a_2). This constitutes the data for our CFD analysis. From a computational viewpoint, the intra-LV flow is determined from the LV wall-motion boundary condition to the standard Potential-flow equation $\nabla^2\Phi = 0$.

The intra-LV pressure gradient can in turn be computed from the unsteady potential flow using the Bernoulli equation.

5.3.2 *Results in characterization of RTF & CONT*

- Figures ($3b_1$ & c_1) depict intra-LV blood-flow velocity distributions during diastole and systole, before nitroglycerin administration
- Figures ($3b_2$ & c_2) depict intra-LV blood-flow velocity distributions during diastole and systole, after nitroglycerin administration
- Figures ($3d_1$ & e_1) depict intra-LV blood-flow pressure distributions during diastole and systole, before nitroglycerin administration
- Figures ($3d_2$ & e_2) depict intra-LV blood-flow pressure distributions during diastole and systole, after nitroglycerin administration

We could interpret the phenomenon as if the LV wall stiffness were providing the resistance to wall-motion for diastole, and the contracting LV were facilitating emptying of the LV during systole, thereby setting up the requisite intra-LV pressure-gradients and velocity distributions. For the patient TURN, Figures (3 d_1 & e_1) demonstrate poor LV-RTF and LV-CONT in terms of adverse intra-LV blood pressure gradients during filling and ejection phases, respectively. However, following the administration of nitroglycerin, these filling and ejection phases' pressure-gradients (and hence LV-RTF and LV-CONT) are improved (Figures 3 d_2 & e_2), thereby providing the basis for advocating coronary revascularization for this patient.

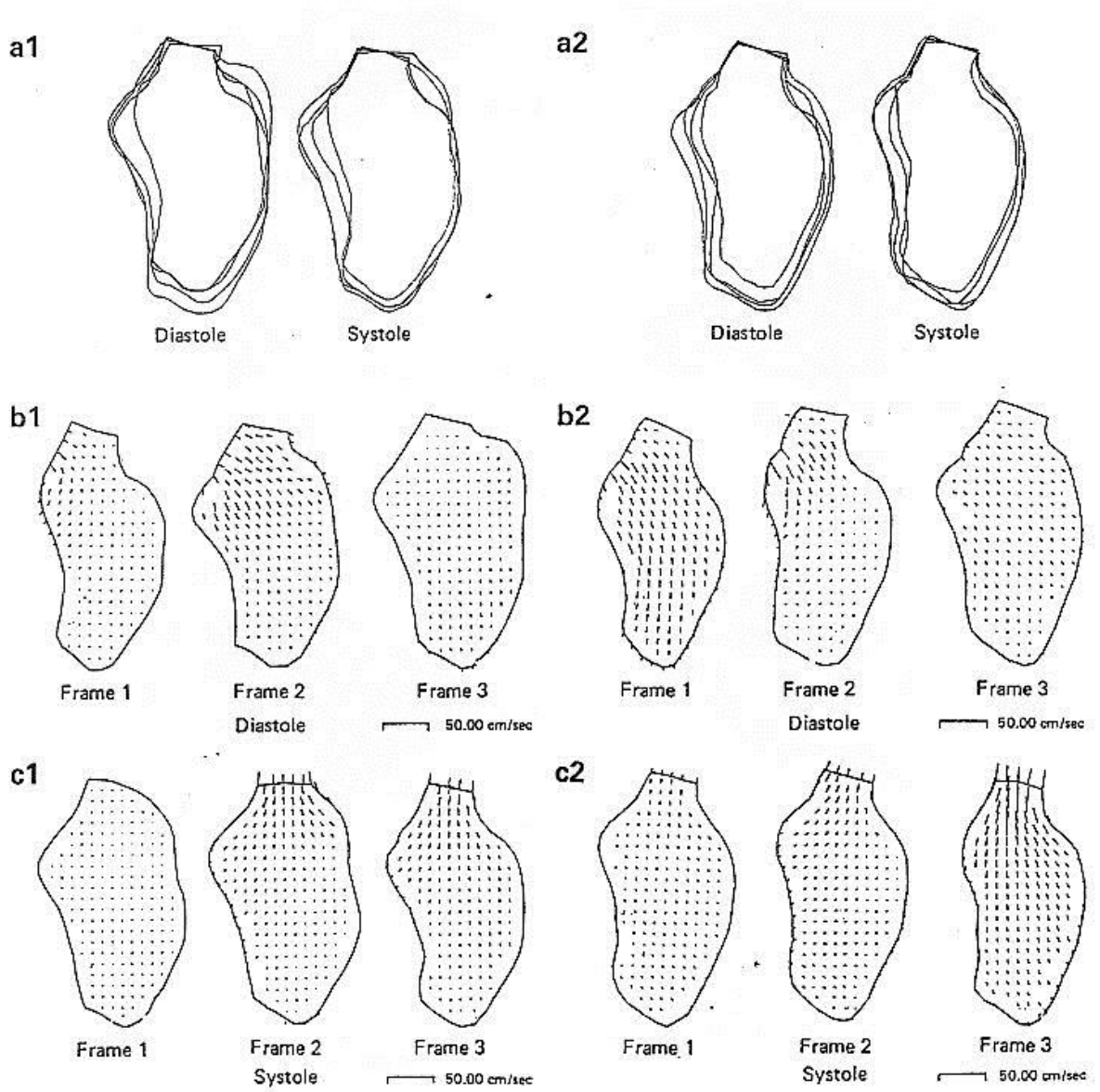

Figure 3: Patient TURN[1] (to be continued on next page) (Ghista, 1987)

[1] The application of finite element methodology to the digitized video-angiographies images during all phases of the cardiac cycle is shown for numbers of patients. A typical patient TURN has severe ischaemic heart disease with large akinetic segments in the anterior and apical wall.

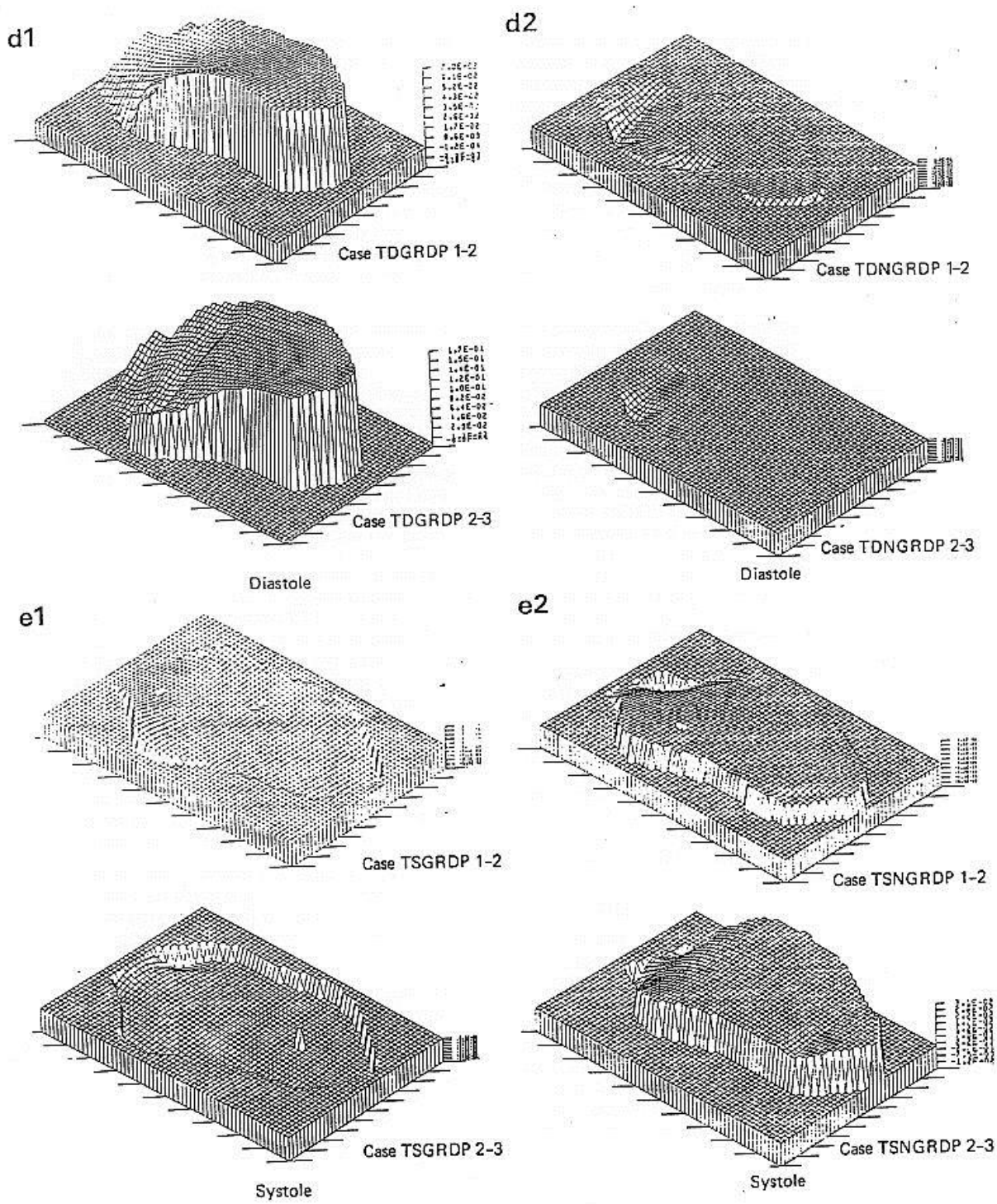

Figure 3: Patient TURN: (a) superimposed sequential diastolic and systolic endocardial frames (whose aortic valves centers and the long axis are matched) before (1) and after (2) administration of nitroglycerin. (b) instantaneous intra-LV distributions of velocity during diastole, before (1) and after (2) administration of nitroglycerin. (c) instantaneous intra-LV distributions of velocity during ejection phase, before (1) and after (2) administration of nitroglycerin. (d) instantaneous intra-LV distributions of pressure-differentials during diastole, before (1) and after (2) administration of nitroglycerin. (e) instantaneous intra-LV distributions of pressure-differential during ejection phase, before (1) and after (2) administration of nitroglycerin. (Ghista, 1987)

6. LV Filling-Performance Index (LVFPI)

Thus far, we have demonstrated the theory, methodology and computation of clinical-diagnostic measures of (i) LV diastolic myocardial stiffness & LV systolic myocardial stress vs. strain-rate, and (ii) LV RTF & LV CONT. The latter set of indices can be applied to decide candidacy for coronary revascularization. A systematic-engineering LV pressure-volume analysis of the diastolic and systolic phases of the cardiac cycle has been carried out, to formulate and evaluate filling and ejection phases' parameters and functional indices.

6.1 Bio-mathematical Model

At the end of isovolumic relaxation, the LV enlarges its volume while its pressure continues to decrease after transmitral flow has commenced. In other words, the model must account for LV suction. A simple explanation of suction is the storage of elastic 'strain' energy in the ventricular wall and surrounding structures during systole, which is recovered and manifested as elastic recoil during diastole (Sabbah, 1981; Robinson, 1986). The LV pressure profile of the ventricular suction has been experimentally demonstrated by Sabbah (1981). After the occurrence of the 'e' wave, the left atrium (LA) starts to contract, and this phenomenon is manifested as the 'a' wave. The model should thus also incorporate this phenomenon.

The diastolic filling can be considered to comprise of two temporal phases. The first phase I, denoted by t_{DV} (and measured in second), corresponds to ventricular passive filling; it comprises the interval from the opening of the mitral valve until the initiation of atrial systole (phase I). This filling is initiated by somewhat explosive LV wall recoil. The second phase II, (t_{DA}), corresponds to the atrial phase of diastole as shown in **Figure 4**. The total duration of diastole t_D is given by

$$t_D = t_{DV} + t_{DA} \tag{1}$$

The contour of a LV volume and flow-rate obtained from cineangiography is shown schematically in **Figure 4**. The flow rate is derived by differentiating the volume with respect to time.

Ventricular diastolic bio-mathematic model (incorporating inertial, resistive and compliant properties) needs to account for both 'e' and 'a' waves, associated with LV suction and LA contraction.

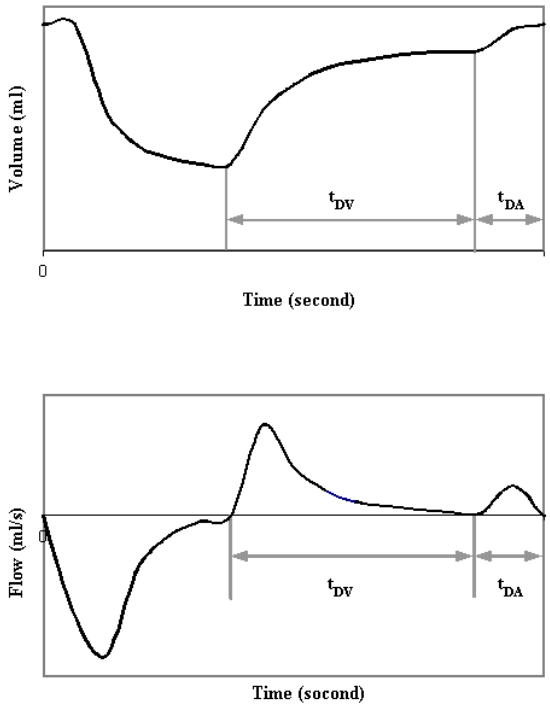

Figure 4: Schematic of LV time curve and first derivative (time-flow curve) via cineangiography. Phase I of diastolic filling occurs for $0 \le t \le t_{DV}$. Phase II encompasses interval $t_{DV} \le t \le t_{DA}$.

From **Appendix A**, the associated governing differential equation (which includes inertial, filling-resistance and compliance terms) is given as:

$$M\ddot{V} + R_e\dot{V} + \frac{V}{C} = F(t) \tag{2}$$

As mentioned earlier, the diastolic filling encompasses two phases. Phase I is passive diastolic filling caused by LV recoil, for which F(t)=0. In phase II, the atrium actively

contract and forces blood into the ventricle, for this process, we assume $F(t) = F_0 \sin(\omega t)$. Our bio-mathematical model represents these phenomena with consideration of the LV volume in responsive to F(t). Intuitively, this can be viewed as the driving term due to the atrial pressure generated by atrial contraction (the 'a' wave).

Phase I: **Early diastolic filling (refer to Appendix B)**.

The over-damped solution for equation (2) is

$$V(t) = V_0 e^{-\alpha t}\left[\frac{\alpha}{\beta}\sinh(\beta t) + \cosh(\beta t)\right] \tag{3}$$

where V_0 is initial volume of LV. $\alpha = R_e / 2M$, $\beta = \sqrt{\alpha^2 - 1/(CM)}$.

Phase II: **Lately diastolic filling (see Appendix B)**

The solution to the equation (2) is

$$V(t_a) = C_3 e^{-(\alpha-\beta)t_a} + C_4 e^{-(\alpha+\beta)t_a} + A\cos(\omega t_a) + B\sin(\omega t_a) \tag{4}$$

where $A = F_0 \dfrac{-\omega R}{M^2(\omega_0{}^2 - \omega^2)^2 + \omega^2 R^2}$; $B = F_0 \dfrac{M(\omega_0{}^2 - \omega^2)}{M^2(\omega_0{}^2 - \omega^2)^2 + \omega^2 R^2}$; $\omega_0 = (1/CM)^{1/2}$

$$C_3 = \frac{(\alpha+\beta)(V(t_{DV}) - A) + \dot{V}(t_{DV}) - B\omega}{2\beta},\ C_4 = \frac{(\beta-\alpha)(V(t_{DV}) - A) - \dot{V}(t_{DV}) + B\omega}{2\beta}$$

6.2 Determination of Parameters for LVFPI

By simulating the volume during phase I with our V(t) solution expressions

$$Vactu = V(t) + (V_{es} - V_0) \tag{5}$$

where V_{actu} is actual volume of LV, V_{es} is end-systolic volume.

We can evaluate the parameters V_0, α and β, as listed in **Table 1**. The model-computed volume matches very well to the data measured, as shown in Figure 5.

Now we will proceed to solve for the remaining parameters: F_0 and ω. During phase II, the solution of *V(t)* must satisfy the following two boundary conditions:

$$V_{actu}(t_{DA}) = V_{ed},\ \dot{V}_{actu}(t_{DA}) = 0 \tag{6}$$

where V_{ed} is end-diastolic volume.

We can further determine the values of F_0 and ω. Hence all model parameters (V_0, α, β, F_0 and ω) can be evaluated. Besides, M equals the mean value of $[\rho h/(4\pi R_e^2)]$ during phase I. Therefore, R_e and C can finally be determined from the equations:

$$R_e = 2\alpha M \ , \ C = \frac{1}{(\alpha^2 - \beta^2)M} \ , \ \text{for over-damped case} \qquad (7)$$

6.3 Results on LVFPI

We apply the above procedure to data as shown in Figure 1 and present the results in Figure 5-a and Table 1. From the volume-time profile, we compute the flowrate-time curve in Figure 5-b, in which we can identify the 'e' wave and 'a' wave.

Let us now interpret the physiological connection to these parameters. High M implies enlarged LV; high R represents mitral stenosis; low C represents stiff LV myocardium; high F_0 means well-contracting LA and low α means normal damping due to normal LV myocardial elastance (Zhong, 2004a).

Table 1: Parameters related to case as shown in Figure 1 during diastolic filling

Parameters	Values	Fitting			Remarks
V_0 (ml)	-57.93±2.33	Volume fit during phase I	RMSE	1.646	This case is classified as the critical mode.
α (s^{-1})	11.11±0.92				
β (s^{-1})	0		R-square	0.99	
M (mmHg/(ml/s^2))	3.66e-6				
R_e (mmHg/(ml/s))	0.81e-4				
C (ml/mmHg)	2212.73				
F_0 (mmHg)	0.36				
ω (s^{-1})	44.132				

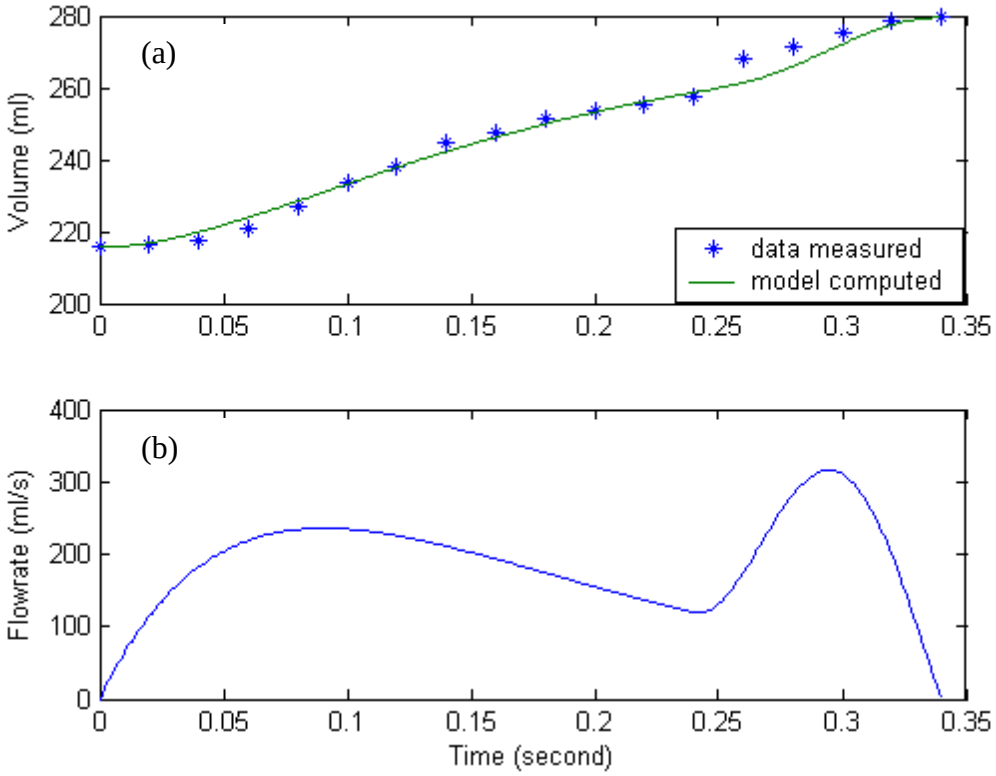

Figure 5: Volume and flowrate for case as shown in Figure 1.

7. LV Contractility Index (LVCI)

7.1 Myocardial Muscle Model

Based on the conventional Hill three-element model (1938) and Huxley cross bridge theory (1957; 1974), we have developed a new myocardial model involving the LV myocardial mass, series-elastic element (SE), viscous-elastic element (VE) and the contractile-element (CE), as shown in Figure 6. We now link the anatomical associations of these myocardial model elements with the microscopic structure of the heart muscle.

Therein, the sarcomere represents the fundamental structural and functional unit of contraction. It is this unit that makes the muscle element contract, distorts its shape and does work within this sarcomere model, where the contractile element (CE) corresponds to the actin-myosin filaments, as presented in Figure 6. The connective tissue between the fibers of the myocardium and the sarcolemma constitute the SE and VE.

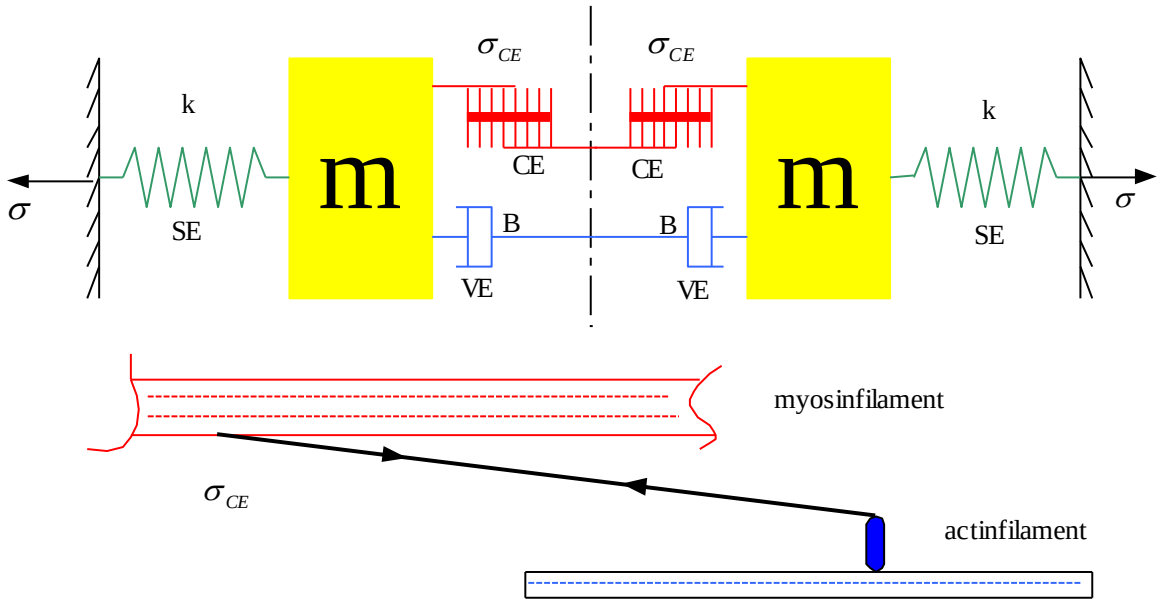

Figure 6: Sarcomere element contractile model, involving: the effective mass (m) of the muscle tissue that is accelerated; elastic parameter k of the series element stress σ_{SE} (k=elastic modulus of the sarcomere element); viscous damping parameter B of the stress σ_{VE} in the parallel viscous element, the generated contractile stress σ_{CE} between myosin (thick) and actin (thin) filaments.

In Figure 6, m denotes the LV myocardial mass, B is the viscosity parameter, k is the elastic-modulus parameter, x_T is the displacement of sarcomere relative to the center line, x_2 is the displacement of the LV sarcolemma, σ_{CE} denotes the stress generated by the CE, σ_{VE} denotes the stress by the VE, σ denotes the resulting total active stress which is related to the chamber pressure of LV.

In this study, the LV is represented as a thick-walled cylinder contracting symmetrically. Transverse isotropy is assumed with respect to the axis of cylinder. The lumped myocardial fiber is depicted in the LV cross-section (Figure 7). The integration of the muscle units causes LV myocardial contraction, as a result of which circumferential active stress is generated per unit area of the myocardium. The active circumferential stress/per unit area acting on the inner surface of the myocardium is denoted by σ.

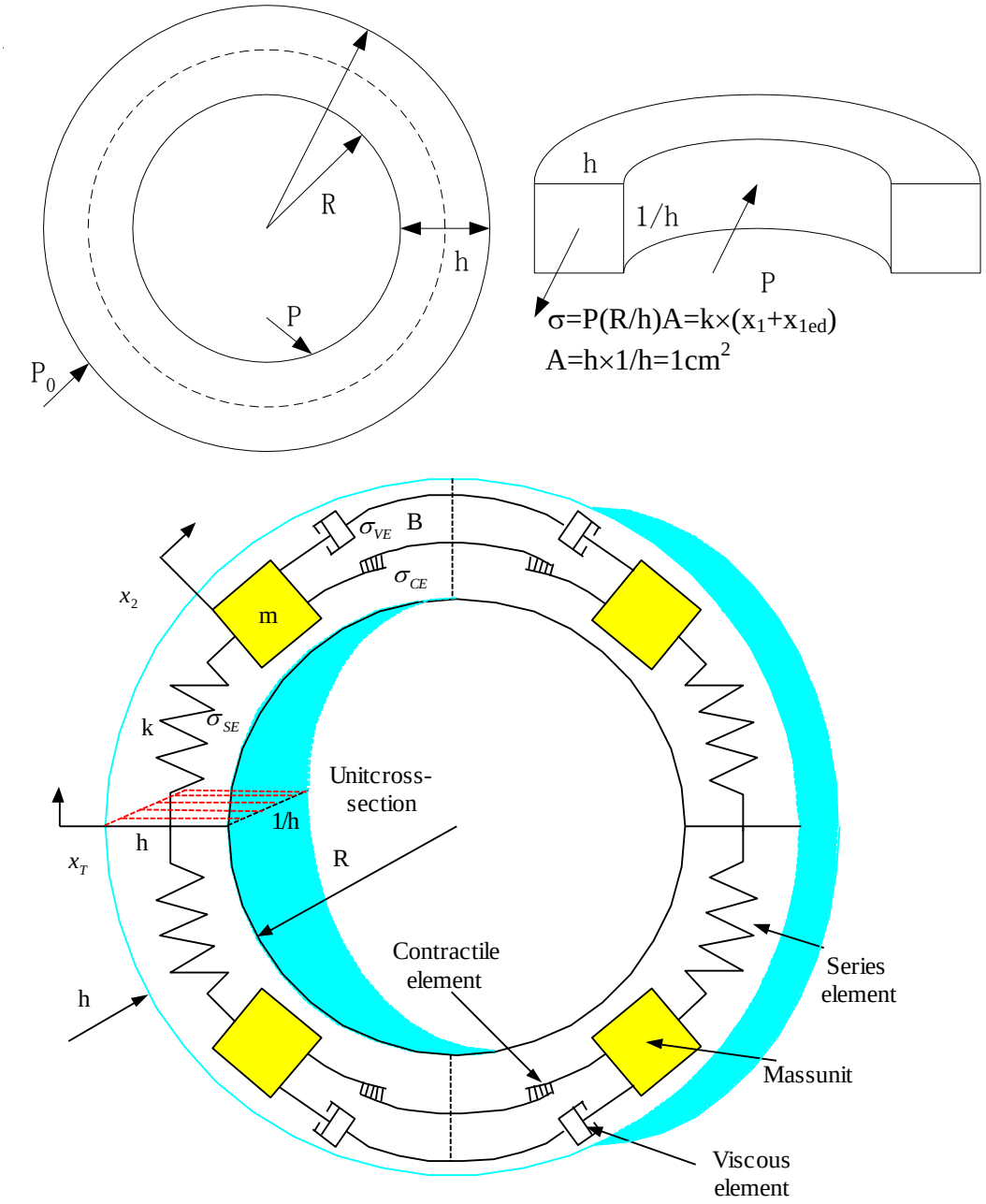

Figure 7: Cross-section of a thick-wall cylinder representing the LV. $\sigma=P(R/h)A$ for simplicity. X_{1ed} is the displacement at the end-diastolic phase.

7.2 Analysis of LVCI

From **Figure 8**, the governing differential equation for sarcomere, due to the generated contractile stress, can be expressed as:

$$m\ddot{x}_2 + B\dot{x}_2 - \sigma_{CE} + kx_1 = 0$$

$$\text{or, } m\ddot{x}_1 + B\dot{x}_1 + kx_1 = \sigma_{CE} - B\dot{x}_T - m\ddot{x}_T \qquad (8)$$

where σ_{CE} is the applied stress exerted by the contractile-element

m is the muscle mass of per unit cross-section area = $\pi R\rho_m / 2$

B is the viscous damping parameter of parallel viscous element

k is the elastic stiffness (or modulus) of SE

x_2 (the displacement of muscle mass m relative to centre-line)= $x_T + x_1$

x_T is the displacement of the muscle half-unit relative to its centre-line

$\sigma_{VE} = B\dot{x}_2$, and $\sigma_{SE} = k(x_1 + x_{1ed})$

Because the term $m\ddot{x}_1$ and $m\ddot{x}_T$ can be neglected due to their small values as compared to other terms. The equation (8) can be rewritten

$$B\dot{x}_1 + kx_1 = \sigma_{CE} - B\dot{x}_T \qquad (9)$$

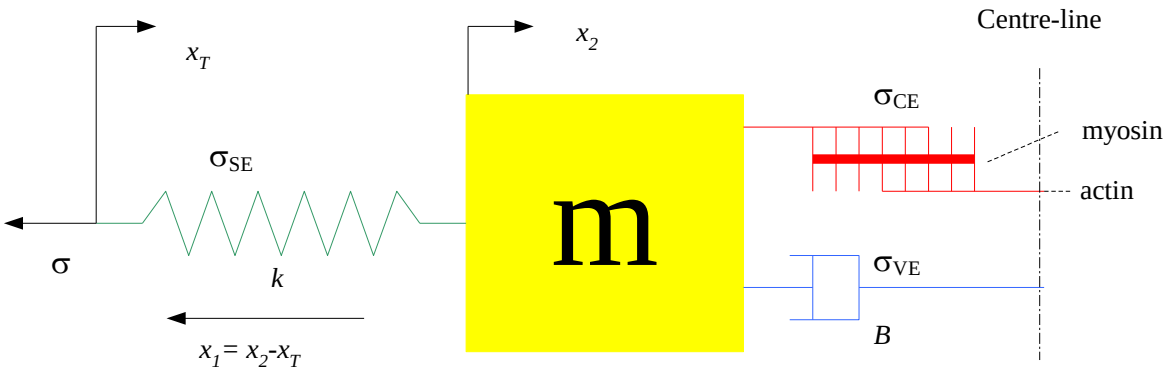

Figure 8: Model for the systolic phase: effective mass (m) of the myocardial sarcomere tissue is mass per unit area; k is the elastic modulus of series element; B is the viscous-damping parameter of parallel viscous element; σ denotes the total generated stress caused by the contractile stress σ_{CE} ; σ_{SE} is the stress in the series element; σ_{VE} is the stress in the viscous element.

The systolic contraction includes two temporal phases. Phase I, denoted by t_{iso} (and measured in second), corresponds to the duration of isovolumic contraction; it comprises the interval from the closing of the mitral valve until the aortic valve open. Phase II, (t_e), corresponds to the ejection phase of systole. The total duration of contraction t_s is given by

$$t_s = t_{iso} + t_e \tag{10}$$

During this phase of systolic contraction, the stress of CE, σ_{CE}, can be considered as (due to LV pressure wave shape)

$$\sigma_{CE} = A_3 \sin(\omega_2 t) e^{-A_4 t} \tag{11}$$

where $\omega_2 = \pi / t_e$, A_3 and A_4 are coefficients.

Phase I: Isovolumic contraction phase (refer to Appendix C):

The solution of equation (9) is given by $x_1 = x_1^{\,c}$.

$$x_1^{\,c} = C_1 e^{-k/Bt} + (a\sin(\omega_2 t) + b\cos(\omega_2 t)) e^{-A_4 t} \tag{12}$$

where $a = \dfrac{A_3(k - A_4 B)}{(k - A_4 B)^2 + (B\omega_2)^2}$, $b = -\dfrac{A_3 B\omega_2}{(k - A_4 B)^2 + (B\omega_2)^2}$, $C_1 = -b$

Phase II: Ejection phase (see Appendix C):

The solution to equation (9) is given by $x_1 = x_1^{\,e}$.

$$\begin{aligned} x_1^{\,e} &= C_2 e^{-k/Bt_a} + (a\sin(\omega_2(t_a + t_{iso})) + b\cos(\omega_2(t + t_{iso}))) e^{-A_4(t_a + t_{iso})} \\ &+ (c\sin(\omega t_a) + d\cos(\omega t_a)) e^{-A_2 t_a} \end{aligned} \tag{13}$$

where $c = -\dfrac{BA_1(k - BA_2)}{(k - BA_2)^2 + (B\omega)^2}$, $d = \dfrac{B^2 A_1 \omega}{(k - BA_2)^2 + (B\omega)^2}$, $C_2 = C_1 e^{-k/Bt_{iso}} - d$

7.3 Determining the Parameters of LVCI

The expression for the LV myocardial stress generated (by σ_{CE}) is then given by

$$\sigma_{SE} = \sigma = k(x_1^{\,e} + x_{1ed}) \tag{14}$$

where $x_1^{\,e}$ is given by equation (13), and x_{1ed} is end-diastolic displacement of SE. The resulting LV intra-cavity pressure P developed (by σ) can then be expressed as:

$$P = \frac{\sigma(R_o^{\,2} - R_i^{\,2})}{(R_o^{\,2} + R_i^{\,2})} = \frac{(R_o^{\,2} - R_i^{\,2}) k(x_1^{\,e} + x_{1ed})}{(R_o^{\,2} + R_i^{\,2})} \tag{15}$$

where R_o and R_i are the outside and inside radius.

By matching the model generated P with the actual LV pressure data of a patient and carrying out parameter-identification accordingly, we can determine the parameters k, B, A_3, and A_4 (as summarized in Table 2). Figure 9-a suggests that the model-computed pressure match the actual pressure very well.

7.4 Power generated by the sarcomere contractile-element

Now, we define the contractile-element power as:

$$Power = F_{CE} \times \dot{x}_2 \tag{16}$$

where (i) both F_{CE} and x_2 being functions of time, (ii) F_{CE}, the contractile force generated by its contractile element, is given by

$$F_{CE} = \sigma_{CE}(h \times 1/h) = \sigma_{CE} \tag{17}$$

(iii) $\dot{x}_2$ is the shortening velocity of the CE, expressed by $(\dot{x}_1 + \dot{x}_T)$.

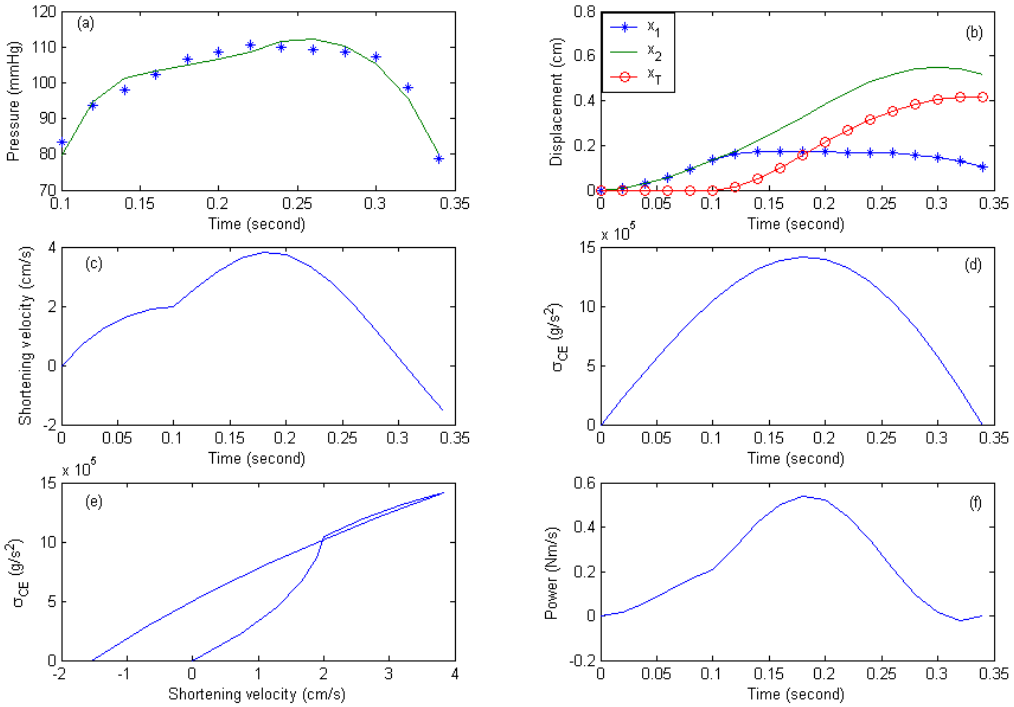

Figure 9: Results for sample case as shown in Figure 1.

7.5 Results of LVCI

Using the values of parameters as presented in Table 2, we have determined and plotted x_1, x_2 and x_T versus time respectively in Figure 9-b. The velocity and CE stress are included in Figure 9-c and 9-d. The power generated by CE is shown in Figure 9-f. The higher the power input, the better will be the contractility. Herein, in quantifying the performance of the LV, contractility is defined as the ability of the LV myocardium to produce a contractile force with a high shortening-velocity capability, so as to exert maximum contractile power (Zhong, 2004b). Accordingly, we define LV contractility index as $Power_{max}$, which in the present sample case is 0.54 Nm/s.

Table 2: Parameters related to case as shown in Figure 1 during ejection phase

Parameters	Values	Fitting		
A_1 (cm)	5.726±0.624	x_T fit during ejection phase	RMSE	0.0421
A_2 (s^{-1})	6.673±0.708		R-square	0.9902
A_3 (g/s^2)	1.184±0.243	Pressure fit during ejection phase	RMSE	2.2690
A_4 (s^{-1})	-1.002±0.778			
B (g/s)	2.596±0.598		R-square	0.9605
k (g/s^2)	3.954±0.867			

8. Conclusion

This paper demonstrates the theory, methodology and computation of clinical-diagnostic measures of (i) LV diastolic myocardial stiffness & LV systolic myocardial stress vs strain-rate, (ii) LV resistance-to-filling & LV contractility, which can be used to decide candidacy for coronary revascularization, (iii) the conventional invasively obtained physiologic variables of diastole, namely: myocardial compliance and resistance-to-filling can be complemented by a quantitative method of cineangiographically volume analysis during

diastolic filling phase noninvasively, and (iv) LV contractile element 'σ_{CE} vs. $\dot{x}_2$' and power generated, which can be viewed as the important LV contractility indices.

In all, we have developed the analysis and procedure to obtain intrinsic characterization of cardiac dysfunction during both diastolic filling and systolic ejection phases. These works provide new ground and insight into the cardiology research.

Nomenclature:

B	viscous damping parameter of parallel viscous element
C	compliance
E	elastic modulus
F_{CE}	myocardial-unit contractile-element force
h	thickness of myocardium
k	elastic stiffness (or modulus) of series element
m	mass per unit cross-section area
m_e	myocardial surface-density or mass per unit surface area
M	$= \rho_s h$
P_{el}	elastic recoil pressure
R	radius of left ventricle
R_e	resistance-to-filling
R_i	inside radius of cylindrical model
R_o	outside radius of cylindrical model
t_a	$=t-t_{DV}$ during diastolic filling; $=t-t_{iso}$ during systolic ejection
t_D	time for diastolic filling
t_{DV}	time for rapid filling
t_{DA}	time for atrial contraction
t_s	time for systolic contraction
t_{iso}	time for isovolumic contraction
t_e	time for ejection
x_1	displacement of series element
x_1^c	x_1 at isovolumic contraction
x_1^e	x_1 at ejection phase
x_{1ed}	end-diastolic x_1
x_2	displacement of muscle mass m relative to centre-line
x_T	displacement of muscle half-unit relative to centre-line
$\dot{\varepsilon}$	strain rate
σ	wall stress
σ_{SE}	stress exerted by the series-element
σ	$= \sigma_{SE}$
σ_{VE}	stress-resistance exerted by the viscous-element
σ_{CE}	applied stress exerted by the contractile-element
ρ	myocardial density
ρ_f	blood density
ρ_s	myocardial surface density
Φ	velocity potential

Abbreviations

CE	contractile element
CFD	computational fluid dynamics
EF	ejection fraction
CONT	contractility
FEA	finite element analysis
2-D	two dimension
LA	left atrial
LV	left ventricular
RTF	resistance-to-filling
SE	series element
VE	viscous element

References:

1. Defares J.G., Osborn J.J. and Hara H.H., 1963, Theoretical synthesis of the cardiovascular system. *Acta. Physiolo. Pharmacol. Neerl.,* 21:189-265.
2. Elzinga G. and Westerhof N., 1972, Pressure and flow generated by the left ventricle against different impedances. *Circulation Research,* 32:178-186.
3. Frank O., Zur Dynamik des Herzmuskels, Z. Biol. 32: 370-447, 1895: Translated into English by Chapman C.B. and Wasserman E. 1959, On the dynamics of cardiac muscle. *American Heart Journal,* 58:282-317 and 58:467-478.
4. Ghista D.N. and Sandler H., 1969, An analytic elastic-viscoelastic model for the shape and forces of the left ventricle, *Journal of Biomechanics*, 2:35-47.
5. Ghista D.N. and Sandler H., 1970, Indirect determination of human left ventricular performance, *Journal of the Association for the Advancement of Medical instrumentation*, 4:242-245.
6. Ghista D.N., Advani S.H., Gaonkar G.H., Balachandran K. and Brady A.J., 1971, Analysis and physiological monitoring of the human left ventricle. *Journal of Basic Engineering*, ASME proceedings, 93:147-161.
7. Ghista D.N., Brady A.J. and Radhakrishnan S., 1973, A three-dimensional continuum analytical (rheological) model of the human left ventricle in passive-active states, Nontraumatic determination of the in vivo values of the rheological parameters, *Biophysical Journal*, 13:832-854.
8. Ghista D.N. and Mirsky I., 1974, Assessment of cardiac function: a mathematical and clinical evaluation, Part 1: Force velocity analyses of isolated and intact heart muscle, *Automedica*, 1:83-91.
9. Ghista D.N., Advani S.H. and Rao B.N., 1975, In vivo elastic modulus of the left ventricle: its determination by means of a left ventricular vibrational model, its

physiological significant and clinical utility, *Medical and Biological Engineering*, 13:162-170.

10. Ghista D.N., Ray G. and Sandler H., 1980, Cardiac assessment mechanics: 1 left ventricular mechanomyocardiography, a new approach to the detection of diseased myocardial elements and states, *Medical & Biological Engineering & Computing*, 18:271-280.
11. Ghista D.N., Ray G. and Sandler H., 1980, Cardiac assessment mechanics: 2 left ventricular mechanomyocardiography, a new approach to noninvasive intrinsic assessment of left ventricular pumping efficiency, *Medical & Biological Engineering & Computing*, 18:344-352.
12. Ghista D.N. and Fallen E.L., 1987, Intrinsic indices of the left ventricle as a blood pump in normal and infarcted left ventricle, *Journal of Biomedical Engineering*, 9:206-215.
13. Grodins F.S., 1959, Integrative cardiovascular physiology: A mathematical synthesis of cardiac and blood vessel hemodynamics. *Quarterly Review of Biology* 34:93-116.
14. Hill A.V., 1938, The heat of shortening and dynamic constants of muscle, *Proceedings of the Royal Society of London Series B*, 126:136-195.
15. Huxley A.F., 1957, Muscle structure and theories of contraction. *Progress in Biophysics*, 7:255-318.
16. Huxley A.F., 1974, Muscle contraction, *Journal of Physiology*, 243:1-43.
17. Little W.C. and Downes T.R., 1990, Clinical evaluation of left ventricular diastolic performance. *Progress in Cardiovascular Disease*, 2:273-290.

18. MacFadden, R.C., Barnes, R.G., Ghista, D.N., Fallen, E.L. and Srinivasan, T.M., 1984, Microcomputer analysis of LV video-angiogram, *Canadian Medical and Biological Engineering Conference*, Ottaea, Canada.
19. Mirsky I., 1976, Assessment of passive elastic stiffness of cardiac muscle: mathematical concepts, physiologic and clinical considerations, directions of future research, *Progress in Cardiovascular Diseases*, XVIII, 4: 277-308.
20. Palladino J.L., Mulier J.P. and Noordergraaf A., 1998: Defining ventricular elastance, *Proc. 20th Int. Conf. IEEE Eng. Med. Biol. Soc.*, Hong Kong, 383-386.
21. Pie Medical Imaging BV 2004 (http://www.piecaas.com, accessed 28 July 04)
22. Pulse Analyzer device, HealthSTATS, 2003 (http://www.healthstats.com.sg accessed 20 July 04)
23. Robinson F.R., Factor S.M., and Sonnenblick E.H., 1986, The heart as a suction pump, *Sci. Am.* 254(6):84-91.
24. Sabbah, H.N. and Stein, P.D., 1981, Negative diastolic pressure in the intact canine right ventricle: Evidence of diastolic suction, Circulation Research, 49:108-113.
25. Sato, T., Nishinaga, M., Kawamoto, A., Ozawa, T. and Takatsuji, H., 1993, Accuracy of a continuous blood pressure monitor based on arterial Tonometry, *Hypertension*, 21(6):866-874.
26. Subbaraj, K., Ghista, D.N. and Fallen, E.L., 1987: Intrinsic indices of the LV as a blood pump in normal and infracted left ventricle, *Journal of Biomedical Engineering*, 9:206-215.
27. Suga H., 1969, Time course of left ventricular pressure-volume relationship under various extents of aortic occlusion, *Japanese Heart Journal*, 11:373-378.

28. Suga H. and Sagawa K., 1974, Instantaneous pressure volume relationships and their ratio in the excised, supported canine left ventricle. *Circulation Research*, 35:117-126.
29. Suga H., 1993, Paul Dudley White International Lecture: Cardiac performance as viewed through the pressure-volume window, *Japanese Heart Journal*, 35: 263-279.
30. Vaartjes S.R. and Boom H.B.K., 1987, Left ventricular internal resistance and unloaded ejection flow assessed from pressure-flow relations: A flow-clamp study on isolated rabbit hearts. *Circulation Research*, 60:727-737.
31. Warner H.R., 1959, The use of an analogy computer for analysis of control mechanisms in the circulation. *Proc. IRE*., 47:1913-1916.
32. Yellin E.L., Nikolic S., and Frater R.W.M., 1990, Left ventricular filling dynamics and diastolic function, *Progress in Cardiovascular Disease* VXXXII No 4: 247-271.
33. Zhong L., Ghista D.N., Ng E.Y-K, Lim S.T., Chua, S.J., 2004a, Left ventricular filling performance index, *Controversies and recent advances in cardiovascular medicine*, Singapore Cardiac Society 16th Annual Scientific Meeting, 69-70.
34. Zhong L., Ghista D.N., Ng E. Y-K, Lim S.T., Chua, S.J., 2004b, Dynamic of contraction of the left ventricle: modeling and application, *3rd Scientific Meeting of the Biomedical Engineering Society*, Singapore, 114-116.

Appendix A: Derivation of Ventricular Diastolic Biomathematical Model

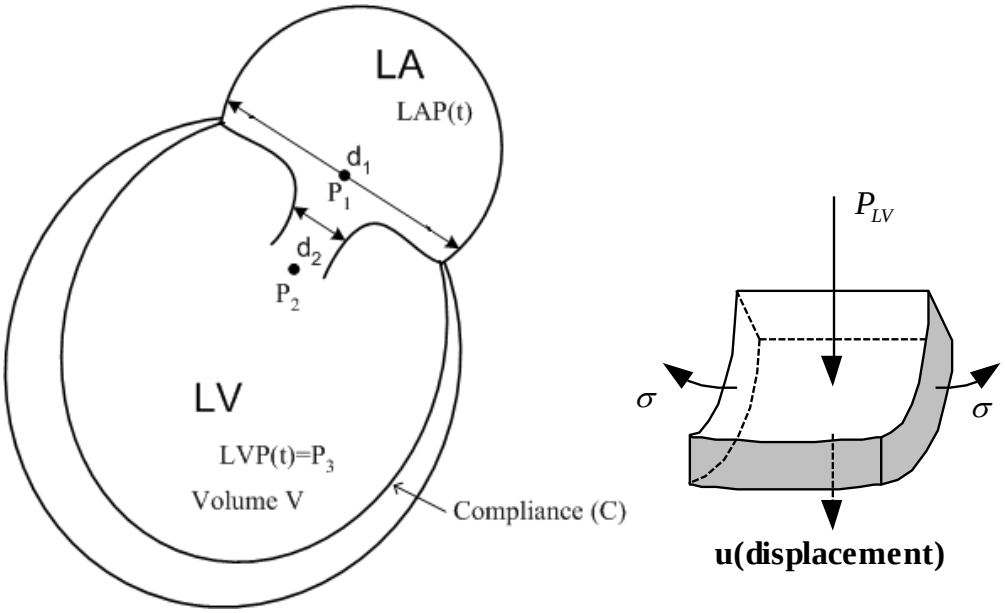

Figure A-1: Dynamic equilibrium of a myocardial element. Element mass $m_e = \rho dxdyh = (\rho h)dxdy = \rho h A_e = m_s A_e$, $\sigma = P_{el} R/(2h)$, P_{el} is elastic recoil pressure. For dynamic equilibrium of the myocardial element, $P_{LV} - P_{el} + m_e \ddot{u} = 0$, or

$P_{LV} - 2\sigma h / R + m_e \ddot{u} = 0$

Dynamic equilibrium of the LV myocardial element gives:

$$m_e \ddot{u} + P_{el} A_e - P_{LV} A_e = 0$$

$$\text{or } m_s \ddot{u} + P_{el} - P_{LV} = 0 \qquad \text{(A-1)}$$

where the myocardial element mass, $m_e = m_s A_e$, m_s (the myocardial surface-density or mass per unit surface area) = ρh, ρ is the myocardial density, and u is the radial displacement (as depicted in Figure A-1).

Now since,

$$m_s = \frac{m_e(element \text{ mass})}{A_e(element \text{ surface area})} = \rho h \qquad \text{(A-2)}$$

$$\Delta V = 4\pi R^2 \Delta u = \dot{V} \Delta t$$

$$\therefore\ \dot{V} = 4\pi R^2 \dot{u}\text{, and } \ddot{V} = 4\pi R^2 \ddot{u} \tag{A-3}$$

we can write:

$$m_s \ddot{u} = \frac{(\rho h)\ddot{V}}{4\pi R^2} = (\frac{\rho}{4\pi R^2})h\ddot{V} = \rho_s h\ddot{V} = M\ddot{V} \tag{A-4}$$

where ρ_s is the surface density, $M = \rho_s h$, and V is the LV volume.

Now, refer to Figure A-1,

$$P_{LA} - P_2 = P_1 - P_2 = R_e \dot{V} \tag{A-5}$$

and

$$P_2 = P_{LV} - \frac{\rho_f v^2}{2} \tag{A-6}$$

where R_e is the resistance to LV filling (through the open mitral-valve), ρ_f is the blood density and *v* is the blood velocity at site 2.

$$\therefore \quad P_{LV} = P_{LA} - R_e \dot{V} + \frac{\rho_f v^2}{2} \tag{A-7}$$

Then,

$$P_{el}\,(\textit{elastic}\text{ recoil pressure}) = P_{el,o} + \frac{V}{C} \tag{A-8}$$

where $P_{el,o}$ is the elastic recoil pressure at the start of filling phase. Hence, from equations (A-1, A-4, A-8), we have

$$M\ddot{V} + \frac{V}{C} = P_{LA} - R_e \dot{V} + \frac{\rho_f v^2}{2} - P_{el,o} \tag{A-9}$$

$$\text{or,} \quad M\ddot{V} + R_e \dot{V} + \frac{V}{C} = P_{LA} + \frac{\rho_f v^2}{2} - P_{el,o} \tag{A-10}$$

So that we can write

$$M\ddot{V} + R_e \dot{V} + \frac{V}{C} = F(t) \tag{A-11}$$

Appendix B: Derivation of LVFPI

Based on **Appendix A**, the associated governing differential equation (which includes inertial, filling-resistance and compliance terms) is given as:

$$M\ddot{V} + R_e\dot{V} + \frac{V}{C} = F(t) \tag{B-1}$$

Rewriting equation (B-1), we have

$$\ddot{V} + \frac{R_e}{M}\dot{V} + \frac{V}{MC} = \frac{F(t)}{M}$$

$$\text{or,} \qquad \ddot{V} + 2\alpha\dot{V} + \omega_0{}^2 V = \frac{F(t)}{M} \tag{B-2}$$

where $\alpha = \frac{R_e}{2M}$, $\omega_0 = \sqrt{\frac{1}{MC}}$ is the natural frequency of the system, α is the attenuation or damping constant of the system, $\beta = \sqrt{\alpha^2 - \omega_0{}^2}$ is the angular frequency of damped oscillation of the system.

Phase I: **Early diastolic filling**

The equation (B-2) becomes

$$\ddot{V} + 2\alpha\dot{V} + \omega_0{}^2 V = 0 \tag{B-3}$$

The relative sizes of the parameters define 3 regimes of motion, which generate a family of solutions to equation (B-3).

The definition of over-damping is that $R_e{}^2 > 4M/C$, hence β is real. Therefore, the solution of equation (B-3) is a product of two real exponentials. If $R^2 = 4M/C$, the solution is referred to as critically damped. If $R^2 < 4M/C$, the solution is referred as an under damped.

Here let us just take over-damped solution for example.

$$V = C_1 e^{-(\alpha-\beta)t} + C_2 e^{-(\alpha+\beta)t} \tag{B-4}$$

For this phase of diastole, the initial conditions that we shall impose are dictated by:

$$V(0) = V_0 = C_1 + C_2 \tag{B-5}$$

$$\dot{V}(0) = -(\alpha - \beta)C_1 - (\alpha + \beta)C_2 = 0 \tag{B-6}$$

Solving equations (B-5 & B-6) for C_1 and C_2 we get

$$C_1 = V_0 \frac{(\alpha + \beta)}{2\beta} \text{ and } C_2 = V_0 \frac{(\beta - \alpha)}{2\beta} \tag{B-7}$$

and hence, the complete expression for equation (B-4) is given by

$$V(t) = V_0 e^{-\alpha t}\left[\frac{\alpha}{\beta}\sinh(\beta t) + \cosh(\beta t)\right] \tag{B-8}$$

Phase II: **Lately diastolic filling**

For mathematical convenience we make a shift in the time variable and redefine it as $t_a = t - t_{DV}$. This changes the limits of our temporal region of interest to

$$0 \le t_a \le t_{DA} - t_{DV} \tag{B-9}$$

The governing equation (B-2) can then be written as

$$\ddot{V} + 2\alpha\dot{V} + \omega_0{}^2 V = F_0 \sin(\omega t_a)/M \tag{B-10}$$

Note that *M*, R_e and *C* may be given different values from their values during phase I of diastole; ω is estimated by the duration of atrial filling. The general solution to equation (B-10) is the sum of the homogeneous and particular solutions, i.e.,

$$V_g(t_a) = V_h(t_a) + V_p(t_a) \tag{B-11}$$

For over-damped case, we obtain from equation (B-11)

$$V_h(t_a) = C_3 e^{-(\alpha-\beta)t_a} + C_4 e^{-(\alpha+\beta)t_a} \tag{B-12}$$

and

$$V_p(t_a) = A\cos(\omega t_a) + B\sin(\omega t_a) \tag{B-13}$$

where

$$A = F_0 \frac{-\omega R}{M^2(\omega_0{}^2 - \omega^2)^2 + \omega^2 R^2}; B = F_0 \frac{M(\omega_0{}^2 - \omega^2)}{M^2(\omega_0{}^2 - \omega^2)^2 + \omega^2 R^2}; \omega_0 = (1/CM)^{1/2}$$

(B-14)

Because the volume changes between phases I and II is continuous, this determines the initial condition for phase II. Hence

$$V_h(0) + V_p(0) = C_3 + C_4 + A = V(t_{DV}) \quad \text{(B-15)}$$

$$\dot{V}_h(0) + \dot{V}_p(0) = -(\alpha - \beta)C_3 - (\alpha + \beta)C_4 + B\omega = \dot{V}(t_{DV}) \quad \text{(B-13)}$$

Solving equations (B-12 & B-13), we have

$$C_3 = \frac{(\alpha + \beta)(V(t_{DV}) - A) + \dot{V}(t_{DV}) - B\omega}{2\beta} \quad \text{(B-16)}$$

$$C_4 = \frac{(\beta - \alpha)(V(t_{DV}) - A) - \dot{V}(t_{DV}) + B\omega}{2\beta} \quad \text{(B-17)}$$

Hence, the complete expression for equation (B-11) is given by

$$V_g(t_a) = C_3 e^{-(\alpha-\beta)t_a} + C_4 e^{-(\alpha+\beta)t_a} + A\cos(\omega t_a) + B\sin(\omega t_a) \quad \text{(B-18)}$$

Appendix C: Derivation of LVCI

Phase I: Isovolumic contraction

Since both the mitral and aortic valves are closed, the volume of blood in the ventricle is constant and pressure inside the ventricle increases. So $x_T = \dot{x}_T = \ddot{x}_T = 0$. The equation (9) becomes

$$B\dot{x}_1 + kx_1 = A_3 \sin(\omega_2 t) e^{-A_4 t} \tag{C-1}$$

The solution of equation (C-1) is given by $x_1 = x_1^{\,c}$.

$$x_1^{\,c} = C_1 e^{-k/Bt} + (a\sin(\omega_2 t) + b\cos(\omega_2 t)) e^{-A_4 t} \tag{C-2}$$

where $a = \dfrac{A_3(k - A_4 B)}{(k - A_4 B)^2 + (B\omega_2)^2}$, $b = -\dfrac{A_3 B\omega_2}{(k - A_4 B)^2 + (B\omega_2)^2}$.

For this phase of contraction, the initial conditions that we shall impose are dictated by:

$$x_1^{\,c}(0) = C_1 + b = 0 \tag{C-3}$$

Solving equation (C-3), we have

$$C_1 = -b \tag{C-4}$$

Phase II: Ejection phase:

For mathematical convenience we make a shift in the time variable and redefine it as $t_a = t - t_{iso}$. This changes the limits of our temporal region of interest to

$$0 \le t_a \le t_e - t_{iso} \tag{C-5}$$

In this phase, x_T is no longer zero, and hence we need to relate it to the LV volume. In this analysis, we assume that the LV is a thick-wall cylindrical chamber of radius *R* and wall thickness *h*. Now we can express x_T in terms of LV model radius *R*, as (refer **Figure 7**):

$$x_T = \frac{\pi}{2}\Delta R = \frac{\pi}{2}(R_{ed} - R(t)) \tag{C-6}$$

By fitting an expression to the [$\frac{\pi}{2}(R_{ed} - R(t))$] clinical data obtained from experiments, we take

$$\dot{x}_T = A_1 \sin(\omega t_a) e^{-A_2 t_a} \tag{C-7}$$

$$x_T = -\frac{A_1}{A_2{}^2 + \omega^2}(A_2 \sin(\omega t_a) + \omega \cos(\omega t_a)) e^{-A_2 t_a} + \frac{A_1 \omega}{A_2{}^2 + \omega^2} \tag{C-8}$$

Hence, the governing equation (9) becomes

$$B\dot{x}_1 + kx_1 = A_3 \sin(\omega_2 (t_a + t_{iso})) e^{-A_4 (t_a + t_{iso})} - BA_1 \sin(\omega t_a) e^{-A_2 t_a} \tag{C-9}$$

The solution of equation (C-9) is given by $x_1 = x_1{}^e$.

$$\begin{aligned} x_1{}^e &= C_2 e^{-k/Bt_a} + (a \sin(\omega_2 (t_a + t_{iso})) + b \cos(\omega_2 (t + t_{iso}))) e^{-A_4 (t_a + t_{iso})} \\ &+ (c \sin(\omega t_a) + d \cos(\omega t_a)) e^{-A_2 t_a} \end{aligned} \tag{C-10}$$

where $c = -\frac{BA_1 (k - BA_2)}{(k - BA_2)^2 + (B\omega)^2}$, $d = \frac{B^2 A_1 \omega}{(k - BA_2)^2 + (B\omega)^2}$

Because the x_T changes between phases I and II is continuous, this determines the initial condition for phase II. Hence

$$\begin{aligned} x_1{}^e(0) &= C_2 + (a \sin(\omega_2 t_{iso}) + b \cos(\omega_2 t_{iso})) e^{-A_4 t_{iso}} + d = C_1 e^{-k/Bt_{iso}} \\ &+ (a \sin(\omega_2 t_{iso}) + b \cos(\omega_2 t_{iso})) e^{-A_4 t_{iso}} \end{aligned} \tag{C-11}$$

Solving equation (C-11), we have

$$C_2 = C_1 e^{-k/Bt_{iso}} - d \tag{C-12}$$